Tribology Online
Japanese Society of Tribologists
https://www.tribology.jp/trol/

Vol. 18, No. 6 (2023) 396-405.
ISSN 1881-2198
DOI 10.2474/trol.18.396

Article

Reducing Friction of Diamond-Like Carbon Film in Sliding through Fluorine Doping

Noor Ayuma Mat Tahir[1)], Shahira Liza Kamis [1)]*, Kanao Fukuda[1)] and Hiroki Akasaka[2)]

[1)] Malaysia-Japan International Institute of Technology, Universiti Teknologi Malaysia,
Jalan Sultan Yahya Petra, 54100 Kuala Lumpur, Malaysia
[2)] Department of Mechanical Engineering, Tokyo Institute of Technology,
2-12-1 O-okayama, Meguro-ku, Tokyo 152-8550, Japan

*Corresponding author: Shahira Liza Kamis (shahiraliza@utm.my)

Manuscript received 31 May 2023; accepted 14 August 2023; published 31 October 2023
Presented at the 9th International Tribology Conference, Fukuoka 2023, 25-30 September, 2023

Abstract

A hydrogenated Diamond-Like Carbon (DLC) film possesses an ultra-low coefficient of friction in a low-humidity environment and higher as the humidity increases. This is due to the presence of water molecules in the atmospheric environment that is physically adsorbed and forming a thick layer on the surfaces that inhibits the growth of carbonaceous transfer film. One viable solution for this problem is to dope fluorine into the hydrogenated DLC film to decrease its surface energy. Therefore, this study varies carbon tetrafluoride feed as a doping source on the hydrogenated DLC film produced via plasma-enhanced chemical vapor deposition on 304 stainless steel substrates. The film hardness, carbon hybridization, and surface hydrophobicity were evaluated using nano-indentation testing, Raman spectroscopy, and contact angle measurement respectively. The coefficient of friction was analyzed by utilizing a ball-on-disc tribometer at a controlled temperature and humidity. The findings suggest that with the increase of the fluorine, the film hardness decreased as the sp^3/sp^2 carbon ratio decreased because weaker C–F bonds are substituting the strong C=C bonds. The increase in fluorine was also observed to produce a more hydrophobic surface. The ball-on-disc test analysis shows that the coefficient of friction was significantly reduced as the C-F bond increased which enables the prevention of carbonaceous transfer film through the adsorption of the water molecule.

Keywords

diamond-like carbon, fluorine-doped, hydrophobic, dry sliding, friction

1 Introduction

Diamond-Like Carbon (DLC) films have received a lot of attention and have been regarded as a next-generation solid lubricating material due to their superior tribological qualities [1,2]. Typically, intrinsic and extrinsic variables both have an impact on the tribological behavior of DLC films. The type of the film is essentially determined by the structural configuration and chemical environments, which take into account the amount of sp^3/sp^2 and heteroatoms; in addition, there is a significant variation in tribological behavior among different DLC films. External variables, such as the substrate material, roughness, sliding circumstances, and surface or interfacial physical and chemical properties of the counterpart surface, might have a significant impact on the tribological behaviors of DLC films [3–7]. In general, chemical bonding, the hardness, elastic modulus, and thermal expansion coefficient of the substrate determine mechanical behaviors like adhesion, elastic modulus, and load bearing for various substrate materials [3, 8–11]. Due to the presence of significant friction and wear, mechanical forces take control of the run when the roughness is high, which was not anticipated to happen. Under various experimental circumstances, the tribological behaviors varied dramatically.

Fluorine-containing, diamond-like carbon (F-DLC) films have received a lot of attention in the last 20 years due to their low surface energy [10, 12, 13], anti-sticking [14, 15], chemical inertness [14], anticorrosion [10, 16], low friction [16], and biocompatibility [10], which makes F-DLC films a promising coating material for a variety of applications. Due to their low friction and low surface energy, ultra-thin amorphous fluorine carbon films (a-C:F) can be employed as an anti-adhesion layer in Micro Electronic Mechanical Systems (MEMS) technology [16]. It is discovered that the characteristics of the C and F components as well as the structures of F-containing DLC films are strongly connected to the features of F-DLC films.

Fluorine has a far higher electronegativity value than both carbon and hydrogen at 3.98. Highly reactive fluorine free

radicals are likely to react with hydrogen compounds during the dissociation of hydrocarbons, resulting in a reduction in the number and/or size of sp^2 graphitic carbon clusters contained in the carbon matrix [10]. The removal of pi electrons and unoccupied electrons, which are the primary polarisation factors, results from the loss of sp^2 bonding. The sum of the polar and dispersive components can be used to express surface energy. The dispersive component of surface energy is an attractive interaction between two nonpolar molecules, while the polar component is dependent on the interaction of dipoles. As a result, it was claimed by previous researchers that adding fluorine to the reactant gas will reduce the surface energy of standard DLC films in half [12, 14].

It is widely acknowledged that environmental factors have a considerable impact on the tribological behaviors of typical DLC films. In dry settings and a vacuum, DLC films have a low friction coefficient, but when the relative humidity (RH) rises, this value tends to rise [4, 5]. This is explained by the fact that water molecules with high polarity are drawn onto the film surface by the polarised C–H bonds in DLC films due to intermolecular interactions. The subsequent layer of water that has been absorbed causes a viscous drag and maybe even capillary forces, which heighten the adhesion and friction of the film surface. The condition is different in ambient or humid situations [4, 17]. DLC films often operate in an air environment, where water cannot be completely avoided. DLC (a-C) films, whether hydrogenated or non-hydrogenated, are extremely sensitive to testing conditions. The coefficient of friction (COF) of hydrogenated DLC films is lower than that of hydrogen-free DLC films in inert or vacuum test settings. As a result, these uncontrollable performances at different humidity conditions will significantly restrict its application in real-world applications.

Fluorine doping into DLC films is first intended to address the weaknesses of traditional DLC films by creating a type of heterogeneous doped amorphous carbon film that can reduce the adhesion forces between the contacting surface under high humidity. Doping fluorine into the DLC films to lower surface energy is one practical solution to this issue. Reduced surface energy, which might diminish intermolecular interactions for the adsorption of water and oxygen, is a result of the polar part's decline. As a result, adding fluorine to DLC films can make such materials' tribological behaviors more environmentally adaptable.

Therefore, it is essential to comprehend the various tribological behaviors of DLC films under various circumstances to bring DLC films to more applications and satisfy genuine requirements. With the consideration of understanding the sliding behavior of different fluorine content doped in the DLC, considerable analysis of the sliding test should be taken and examined films as closely as possible. The behavior of tribology may, in the end, be precisely and rationally tailored from a chemical standpoint. Thus, this study aimed to evaluate the tribological effect of different fluorine content in a controlled environment.

2 Experimental setup

2.1 DLC preparation

The diamond-like carbon film was fabricated by using Plasma Enhanced Chemical Vapor Deposition (PECVD) with stainless steel grade: JIS SUS304 as its substrate. The substrate was first grind until mirrored surface and cleaned with a mixture of hexane and ethanol (1:1) for 10 minutes in an ultrasonic bath. In this study, the doping agent selected was Carbon Tetrafluoride of Tetrafluoromethane (CF_4) was varied at 0, 3, 5, and 10 sccm while other parameters are kept constants for all samples. The inert gas used to purge oxygen in the chamber was Argon (Ar), the interlayer source used to adhere film with the substrate was Tetramethylsilane (Si $(CH_3)_4$) or called TMS, and the carbon source used to deposit is Acetylene (C_2H_2). The schematic diagram of the PECVD and deposition conditions are summarized in Fig. 1 and Table 1.

2.2 DLC characterization

The element content on the DLC coatings was determined by using EDX analysis on 5 ×50 magnification images at 4 different areas for each sample. The coating thickness was obtained by using a non-contact profilometer. A non-contact profilometer scans and measures topographic features using optical light interference principles. As a result, a non-contact optical profilometer can trace the surface topography without harming the real surface features which include

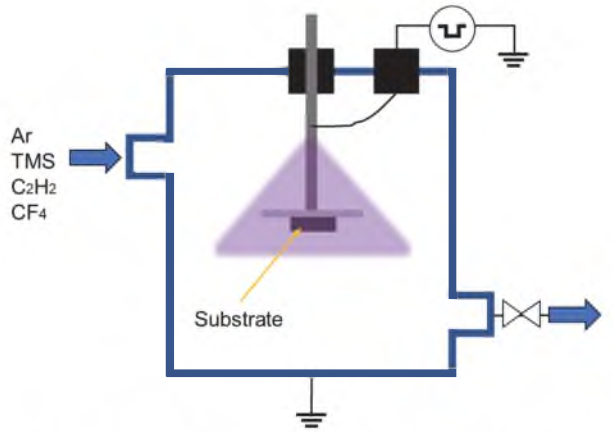

Fig. 1 Schematic diagram of the PECVD to synthesize DLC

Table 1 Parameter used to synthesize DLC

	Ar	TMS	C_2H_2+CF_4	CF_4
Flowrate [sccm]	20	10	10	0, 3, 5, 10
Pressure [Pa]	5	3	3	
Applied Voltage [kV]	2.5	10	10	
Frequency [kHz]	10			
Duty Cycle [%]	5			
Time [min]	30	15	45	

coating thickness and surface roughness. Raman spectroscopy with the green light of 532 nm wavelength was utilized to determine the carbon hybridization of all films. With the aid of Origin software, baselines were constructed to normalize the spectrum before analyzing the peaks; D and G peaks. The film hardness was measured by using a nano-indentation test where 6 repeated measurements were made for each sample. By utilizing a 115° tip, the indentation was maintained under 10% of the film's thickness. The measurement was made 6 times at different spots for each sample to ensure the uniformity of the data collected. Lastly, the hydrophobicity of the film was determined by using a contact angle using distilled water with 3 times repetition on each surface. The image was captured within 3 seconds of drop and analyzed by using the Java-based software ImageJ.

2.3 Tribological characterization

The tribological performances of the sample were investigated with a ball-on-disc tribometer. The counterpart was an 8 mm JIS SUJ2 (G4805 steel) polished up to surface roughness, Ra 0.02 μm. The test was performed at a constant sliding speed of 104.72 mm/s, an applied load of 1 N, and 2000 rotations under a controlled environment. The temperature and humidity are controlled through (temperature 24 ± 1°C, and humidity 58 ± 1%). The schematic diagram of the ball-on-disc is shown in Fig. 2. The wear rate is determined by using Archard's Equation where it is defined as the volume loss (volume of removed material) at a unit load and sliding distance. The volume of removed materials is obtained from the wear area calculated from the wear track using the non-contact profilometer and multiplied by the wear circumference. To understand more about how the wear mechanisms of the formation and failure of the tribo-layer, data obtained during the ball-on-disc test were used to form a spatiotemporal analysis. The analysis works by collecting the dynamic synchronized clock signals from a rotary encoder equipped with a rotating shaft for driving disk specimens. With this mechanism, the dynamic data can be collected as the number of repeated sliding and sliding positions and then mapped on the spatiotemporal plane [17, 18].

3 Results and discussion

Starting from this point onwards, the undoped DLC will be referred to as 0F-DLC, meanwhile, the doped DLC will be referred to as #F-DLC as the # representing the 3, 5, and 10 sccm flow respectively. The element analysis of the DLC is shown in Table 2 where it is confirmed that there were no external elements besides carbon and oxygen were observed on the 0F sample meanwhile the Fluorine element increased as the flow rate increased.

3.1 Mechanical properties

The surface roughness (Ra) of the coatings is almost the same for all coatings. However, there are decrease trends observed as the fluorine content increased with 0.1585, 0.1351, 0.1080, and 0.0713 μm for 0F, 3F, 5F, and 10F respectively with standard deviations less than 0.02. Meanwhile, the film thickness measured for the coating is relatively the same for all samples; 1.6 ± 0.1 μm. With consideration of indentation depth should not exceed 10% of the coating thickness to eliminate the influence of substrate hardness, the indentation depth was pre-set at 0.065

Table 2 Element content in DLC

sample	element	average weight%
0F	C	98.47
	F	0.00
	O	1.53
3F	C	93.62
	F	5.30
	O	1.08
5F	C	91.81
	F	7.21
	O	0.98
10F	C	85.70
	F	13.47
	O	0.83

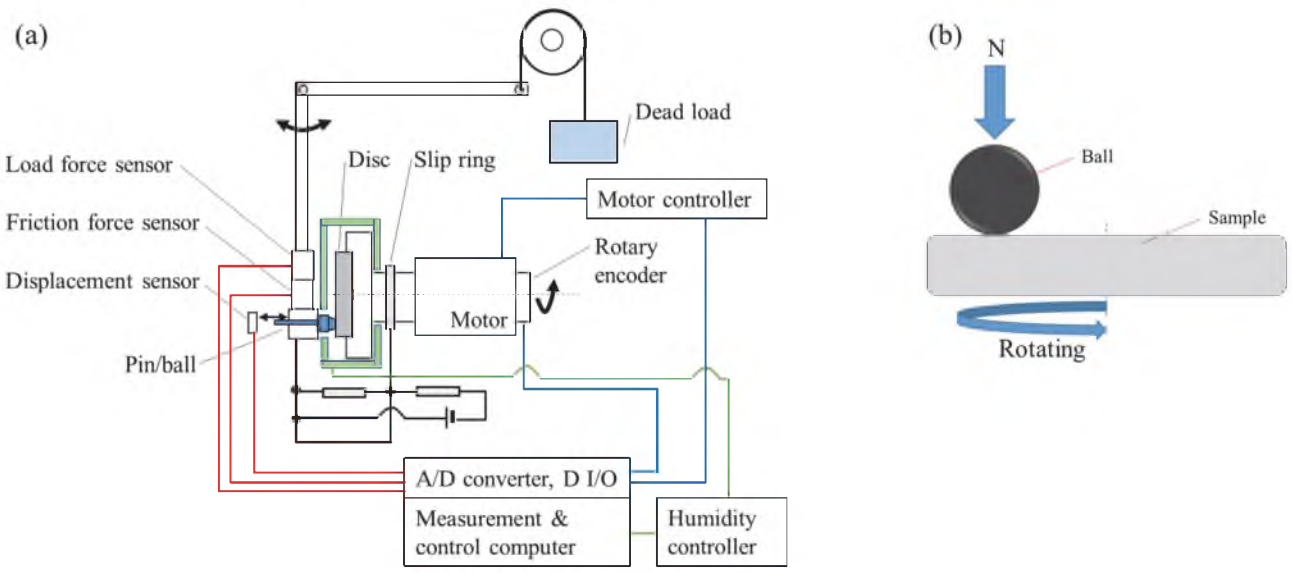

Fig. 2 Schematic diagram of (a) ball-on-disc tribometer, and (b) closeup schematic of the ball and disc

μm (around 4% of the coating thickness) for all samples. The obtained hardness (H) and Young's modulus (E) of the films are represented in Fig. 3. The reported value was represented in the graph as its average and standard deviation as its error bar.

It is noted that both the hardness and Young's modulus of the films decrease as the fluorine content increases. The 10F-DLC reduced around 16.8% and 5.6% of hardness and Young's modulus respectively compared to the 0F-DLC film. This reduction can be attributed to the C–F formation, replacing the C=C bonds. It was discussed by earlier research that the C–F bonds are weaker than the C=C bonds and thus reflecting the finding in Fig. 3. The hardness of DLC films is attributed to the C–C network. This network was disrupted by F which decreased the cross-linking. This disruption creates a more open structural arrangement which eventually leads to lower hardness and Young's modulus [19].

3.2 Carbon hybridization and hydrophobicity

It is well known that a typical Raman spectrum of DLC is composed of G and D bands, in which the G band centered approximately around 1530~1580 cm^{-1} is due to the symmetric E_{2g} vibrational mode in graphite-like materials and the D band at approximately around 1300-1350 cm^{-1} comes from the limitations in the graphite domain size induced by grain boundaries imperfections [20, 21]. To reveal the microstructural changes of F-DLC with various fluorine content, the peak position of all the Raman spectrums was determined by Gaussian fitting with a maintained reduced-chi square between 0.99 to 0.96. The analysis data for each sample are limited in the 1200~1800 cm^{-1} region as shown in Fig. 4 meanwhile Fig. 5 shows the effect of fluorine doping content on the full-width half maximum (FWHM) and peak shift for the G band, along with the intensity ratio of D against G band (I_D/I_G).

Figure 4 shows the Raman spectrum observed for all deposited DLC films. The thick black line represents the actual spectroscopy observed, the red line represents the cumulative fitted peaks, the blue line represents the D band, and the green line represents the G band. Please note that only the spectrum before sliding will be discussed whereas the spectrum after sliding will be discussed in the next section: Tribological performance.

By standardizing the intensity scale, it can be seen that the intensity for both bands is low at the 3F-DLC and increases as the fluorine-doped content increases. It was discussed by previous research that there are several possible factors that can vary the intensity such as crystal orientation, stretching of heavy atoms, and polarization [22–24]. Similar findings can be observed from previous studies where the intensity increased as the doping agent content increased [25]. Detailed alterations of the alterations of crystal orientation, atom stretching, and polarization were discussed next. Ferrari and Basko [22] discussed that the intensity was actually due to the presence of interference that affecting the sum over k value, where k is the electronic wave vector, with or without the phonon energy. They also explained that doping rate can alter the occupancy of electronic state. This is because Pauli blocking prevents the transition from an empty state to a filled state. The doping can effectively prevent specific areas of k from contributing to the matrix element. This interference causes the intensity to increase at high doping rates due to the suppression of destructive interference. This interference was predicted by Basko [26] and demonstrated by Chen et al. [27] which are aligned with this study finding. Pauli blocking happens when fermions in a gas are packed so closely together that every possible quantum state is taken up, a condition of matter known as Fermi Sea. When that occurs, the particles lose their ability to move, making it impossible for light to provide them velocity.

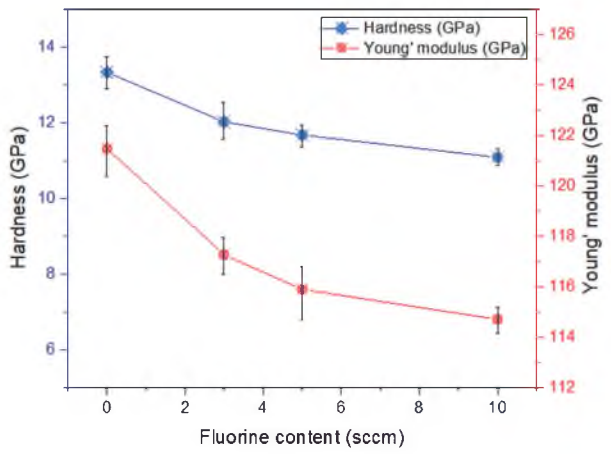

Fig. 3 Hardness and Young's modulus of DLC at different fluorine content

Overall, all films show lower G band intensity compared to D band intensity. Quantitative analysis of the Raman spectrum in Fig. 5 shows that the FWHM(G) decreased as the fluorine content increased, meanwhile, the Peak shift (G) shows an upwards tendency compared to the undoped DLC film. The intensity ratio of the D and G band (I_D/I_G) increases with the increase of fluorine. This trend indicates a decrease in the sp^3/sp^2 ratio that indicates the films became more graphitic. A similar trend was also reported in other studies [14, 28]. It was suggested by Yao et al. that the cross-linked C–C bond in DLC film was broken and the sp^3 diamond matrix would be collapsed when fluorine was introduced into the film [14]. As a result, the fluorine-doped film has more sp^2 carbon domains. The formation of C–F stands out from the C–C network and disturbs the local carbon microstructure by forming big rings and chains, as was also noted by earlier researchers, who found that F and C could only create a single bond [28]. Rings near the edge of the C–C network began to interlock more easily as the F content rose, providing the formation of a structure resembling a polymer. Fluorine doping causes the sp^3/sp^2 ratio to decrease, which causes the DLC film to take on the characteristics of a polymer-like.

The hydrophobicity of the film was determined by contact angle testing which measures the angle between a liquid interacting with a solid surface. Distilled water (H_2O) was selected as the representative for polar liquid. The contact angle comparison for all films was shown in Fig. 6.

From the graph comparison in Fig. 6, the contact angle observed for all surfaces by using distilled shows an increasing pattern as the fluorine content increased. Due to the polar nature of water and the fact that polar liquids only interact with polar surfaces and dispersive liquids only interact with dispersive surfaces, polar liquids have contact angles that are highly sensitive to the polar component of surface energy. The observed contact angle increased by 2.8, 9.5, and 18.3% for 3F, 5F, and 10F-DLC respectively. Since fluorine is non-polar, it limits the dispersion of water on the film surface. Thus, as the fluorine content increases, the dispersion of water is decreased. In other words, it can be said that the increase in fluorine content led to the hydrophobicity of the DLC surface.

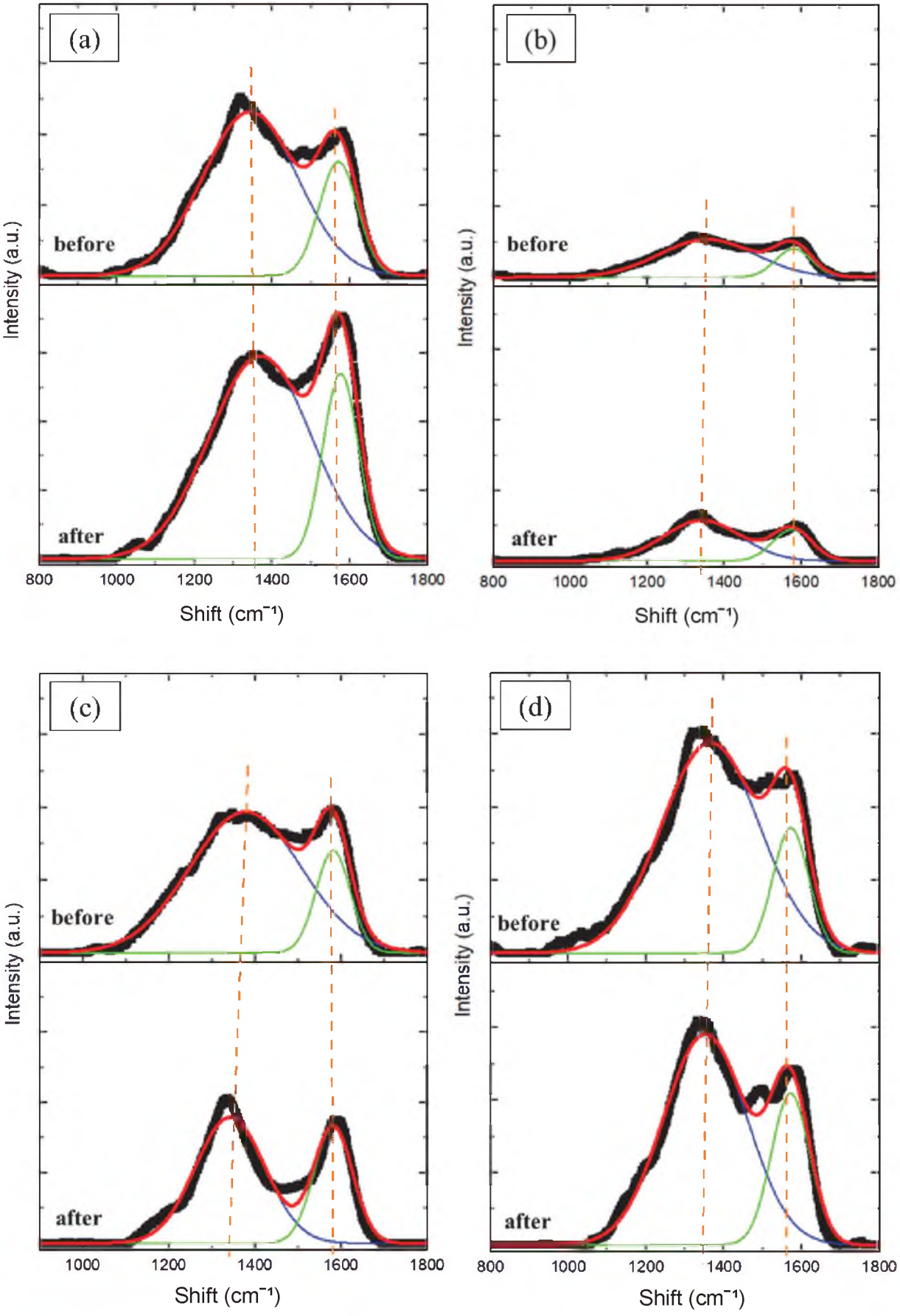

Fig. 4 Raman spectroscopy observed before and after sliding for (a) 0F, (b) 3F, (c) 5F, and (d) 10F-DLC

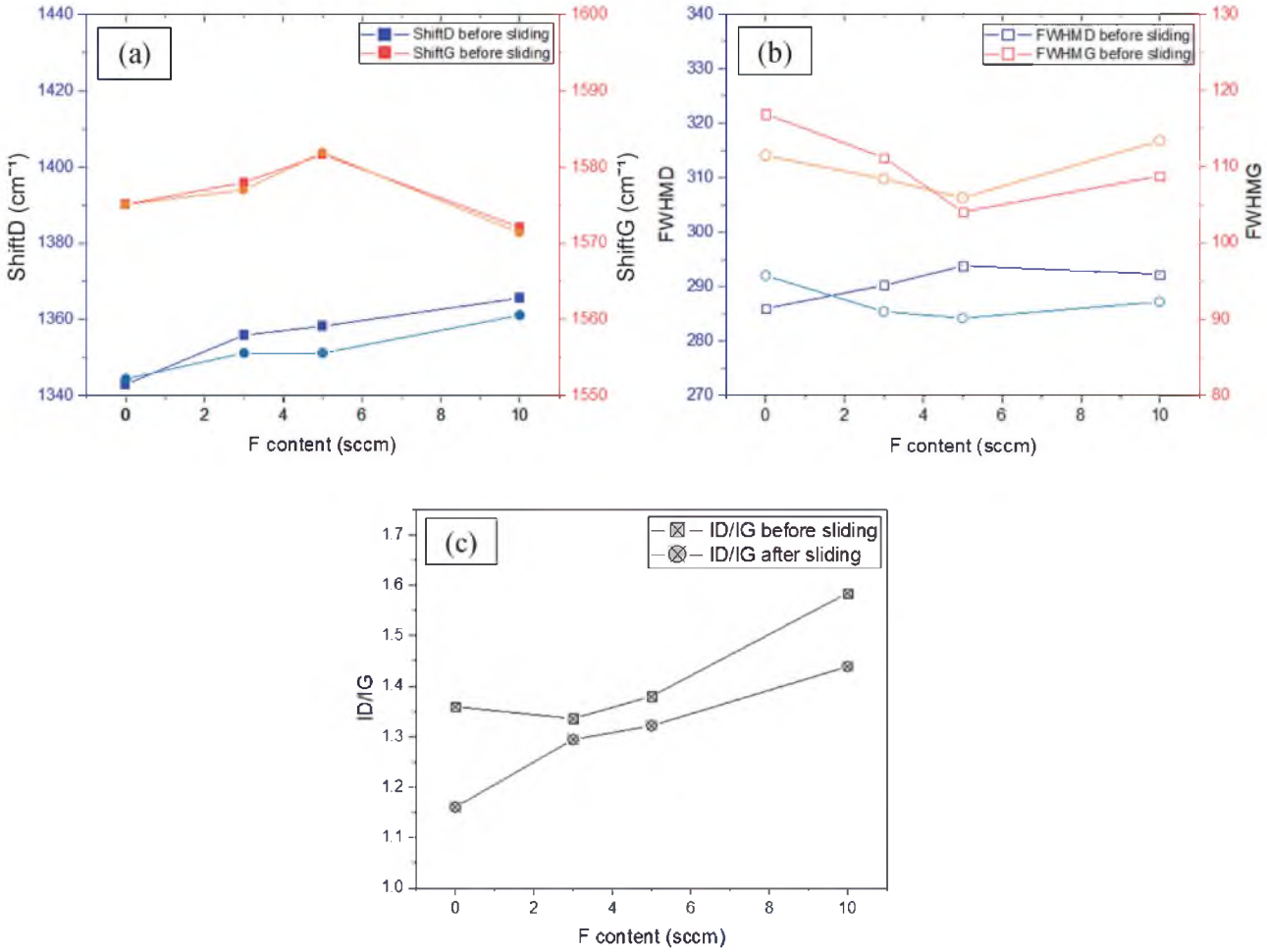

Fig. 5 Analyzed peak from the spectroscopy for (a) FHWM(G) and Peak Shift (G), and (b) I_D/I_G ratio of DLC at different fluorine content before and after sliding

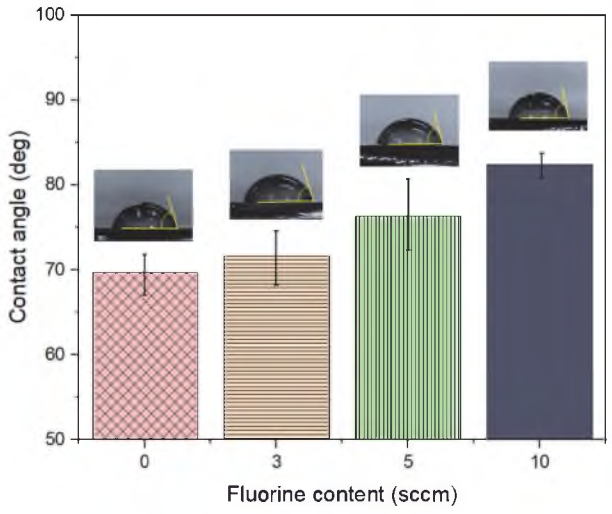

Fig. 6 Contact angle comparison of DLC at different fluorine content

3.3 Tribological performance

As discussed earlier, the increase in fluorine content decreases the sp^3/sp^2 ratio by replacing the strong C–C bond with a weaker C–F bond. As a result, the hardness and Young's modulus decreased. On the other hand, the presence of the C–F bond was concluded by several studies to be beneficial in promoting the hydrophobicity of a DLC film surface. This was proven by the water contact angle test observed earlier. An interesting trend was found in the DLC film study where it was able to provide the lowest coefficient of friction (COF) in open air compared to in vacuum. In this study, the COF of undoped- and doped-DLC films were studied by using a ball-on-disc sliding tribometer under controlled humidity at 58%. The humidity was determined by the average of local humidity condition. Manaf et al. [29] that the formation of water layer varies depending on the surface conditions such as surface roughness, pores, and defects. In this study, all films are free from cracks and pores in upon the preliminary inspection. It was also discussed that even at normal condition (35 – 75% RH), the formation of adsorbed water layer is different depending on the surface conditions. The sliding speed and load tested are 104.72 mm/s and 1 N respectively, for 2000 rotations. The comparison of COF for the tested films is shown in Fig. 7(a) meanwhile the comparison of average COF and wear were shown in Fig. 7(b). The spatiotemporal mapping analysis on the sliding test to support the finding is shown in Fig. 8

meanwhile the SEM image of the worn surfaces is shown in Fig. 9. Spatiotemporal mapping analysis is an analysis technique developed by our laboratory to observe the contact behavior during the ball-on-disc test. Each rotation contains 720 data points collected. The data were then interpreted into the binary color index (black and white). The black represents low friction force meanwhile white represents high friction force. Then, by stacking each rotation's data, mapping analysis is created and allows us to interpret the sliding behavior easily and clearly.

Figure 7(a) shows the COF trends sample based on the number of rotations. In this study, the number of rotations was fixed at 2000 rotations for each sample. With a data repeatability of three for each film, the average COF was then calculated and plotted against fluorine content. From the COF graph against rotations, the trends are very much different, especially for the 10F-DLC where it is inversely with others. Based on the spatiotemporal mapping (in Fig. 8) and wear images (in Fig. 9) observed, we decided that the film starts to wear off at around

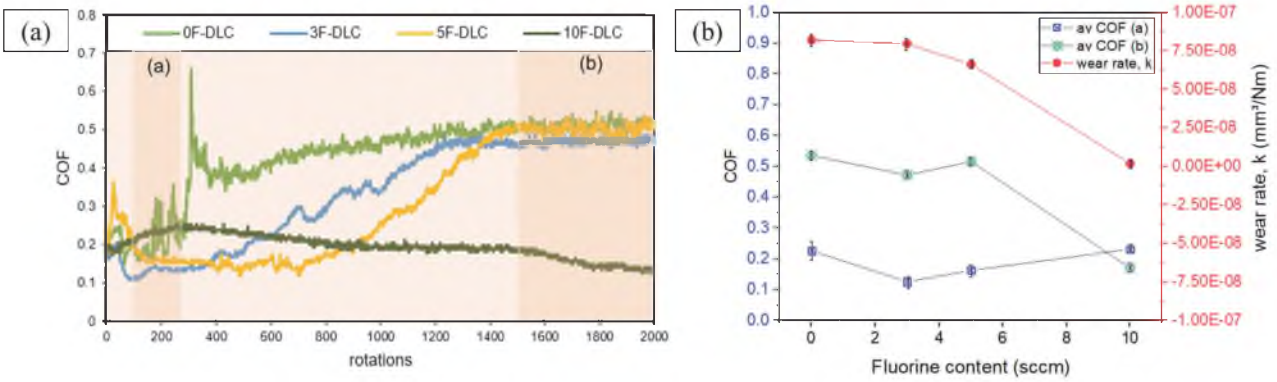

Fig. 7 Comparison of (a) COF trends of different fluorine content against rotations, and (b) average COF and wear rate of DLC at different fluorine content

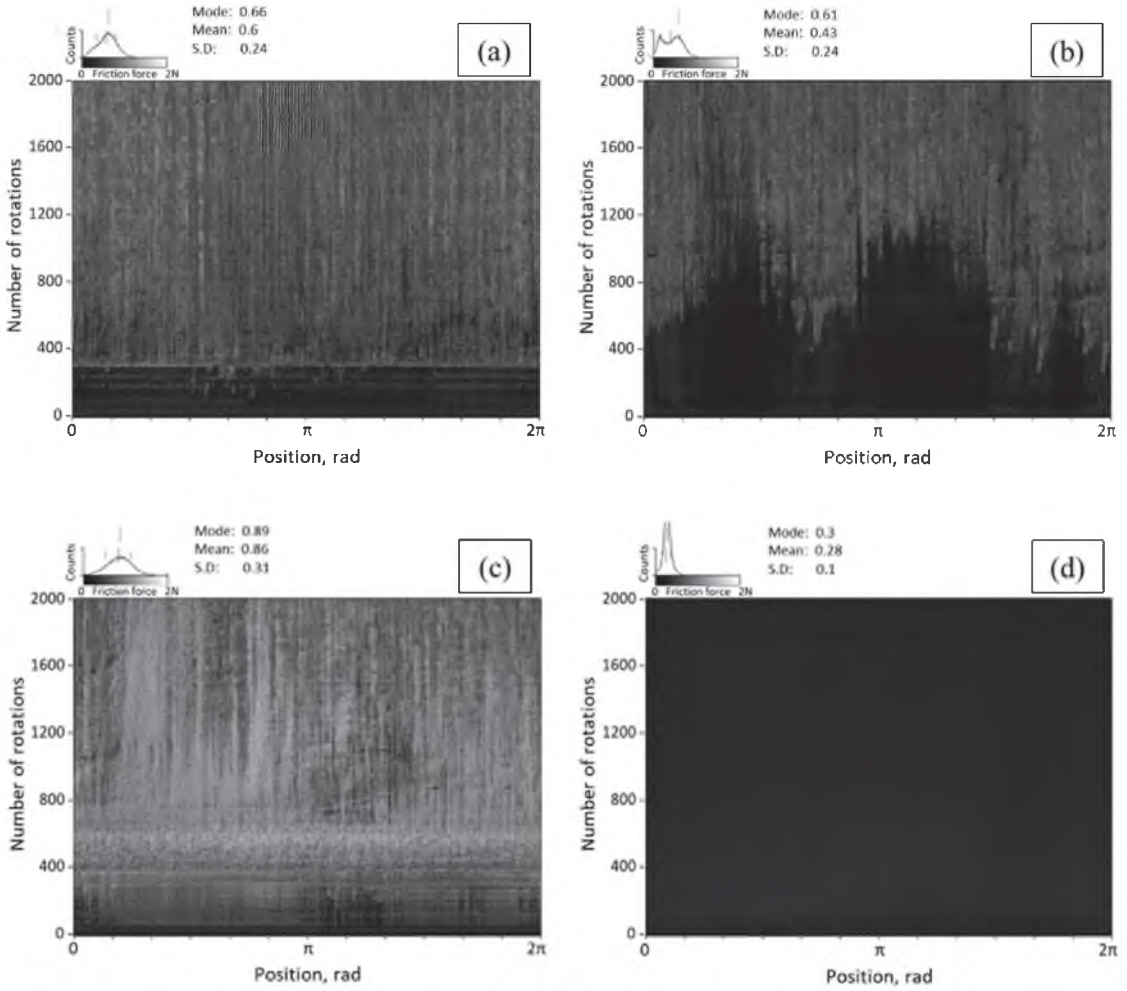

Fig. 8 Friction force spatiotemporal mapping images of (a) 0F-DLC, (b) 3F-DLC, (c) 5F-DLC, and (d) 10F-DLC

the 280-310th, 390-430th, and 800-830th rotation for 0F, 3F, and 5F-DLC. Meanwhile, the 10F-DLC films are still not worn off until the 2000th rotation. Besides the consistent data shown in the COF graph, the spatiotemporal mapping shows no color changes indicating that there is no failure of film for the 10F-DLC, unlike the other films.

From the observations, we decide to analyze two areas, which we consider as before the film wore off (a) and after the film wore off (b). Figure 7(b) shows a clearer COF behavior of the films in region (a) and region (b). For region (a), the COF for all samples is between 0.12~0.24 with 3F-DLC being the lowest and 10F-DLC being the highest. In this region, it was believed that the film is not yet to be worn off. The spatiotemporal analysis shows no significant changes in friction force. Here, it is suspected that the fact that the polarized C–H bonds in DLC films absorb water molecules, which have great polarity, onto the film surface through intermolecular forces. The resulting water-adsorbed layer leads to a viscous drag and even capillary forces, thus increasing the adhesion and friction of the film surface [15]. As a result, the COF of 0F-DLC is higher compared to 3F and

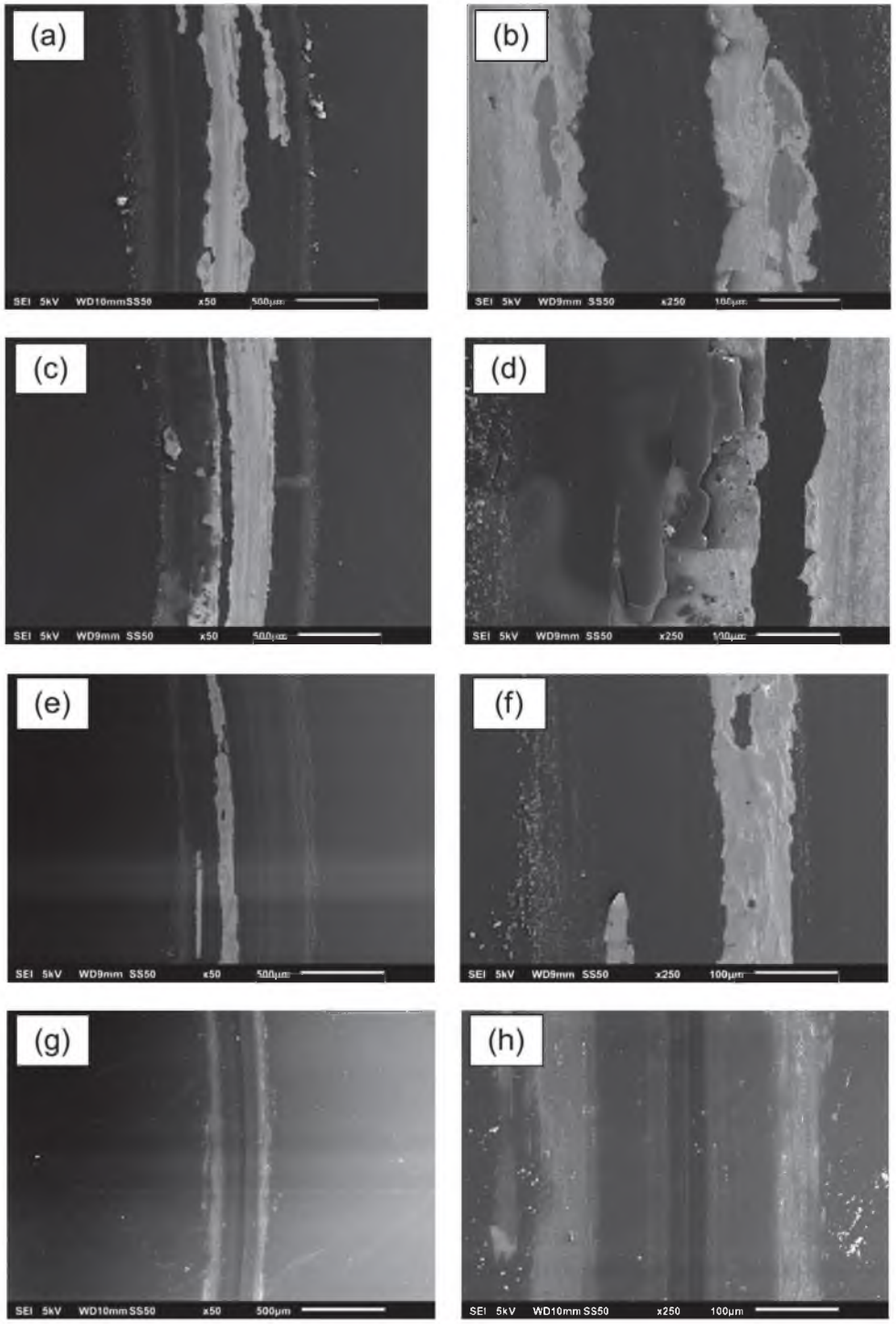

Fig. 9 Worn image of (a-b) 0F-DLC, (c-d) 3F-DLC, (e-f) 5F-DLC, and (g-h) 10F-DLC at ×50 and ×250 magnifications respectively

5F-DLC. Similar trends were observed for region (b) except for the 10F-DLC where it decreases further and reached a COF of 0.17. The 0F-DLC film has the highest COF with around 0.54, followed by 5F at 0.52, and 3F-DLC at 0.47. Here, it was believed that the 10F-DLC film has not worn off and is believed to be able to further lower the COF before it wears off. The presence of a C–F bond on the film surface enhances the hydrophobicity of the surface. The decrease of the polar part contributes to the reduction of surface energy, which can lessen the intermolecular forces for the adsorption of water and oxygen. Therefore, fluorine doping in DLC films can improve the environmental adaptability of their tribological behaviors. As a result, the 10F-DLC can maintain low friction throughout the sliding test. Besides that, the metal countersurface that is attracted to a polar part allows the adhesion of wear debris on the surface, promoting the formation of transfer films which eventually promotes the sliding between the ball and film. Consequently, the coefficient of friction reduces as the rotations increase.

The analysis of the carbon-fluorine bonding with various fluorine contents was done by Bendavid et al. by using an X-ray photoelectron spectroscopy (XPS) spectrum of the C1s peaks. They clarified that there are C–CF, and C–F groups when the fluorine level is less than 20%. They also added that when the fluorine level hits 23%, CF_2 groups start to form, and the structure changes from a diamond-like structure to a polymer-like structure. Besides that, researchers hypothesized that an increase in C–F bonds correspond to a decrease in C=C bonds [12]. Due to the inductive influence of the fluorine atoms, the conjugated C=C bonds produce electron-deficient carbon through polarized σ bonds, and such an electron-deficient carbon receives electrons into the σ^* anti-bonding orbital by the nucleophilic attack. As a consequence, the C=C bond is broken. In conclusion, the formation of C–F, and C–CF bonds allows F-DLC films with low fluorine concentrations (in this case 3F and 5F-DLC) to maintain the diamond-like structure. High fluorine concentrations, however, cause these films to exhibit a property of polymer-like structural organization, which is a result of the interaction of two factors. The carbon network is first disrupted by the appearance of CF_2 groups as significant rings and chains. The formation of sp^2 hybridized carbon domains in the microstructure which is reflected by the shift of G peaks to a higher frequency (refer to Fig. 5a).

The worn surface in Fig. 9 shows the severity of the film worn after 2000 rotations. Figure 9 shows the worn surface of 0F-DLC for ×50 and ×250 magnification for 0F, 3F, 5F, and 10F-DLC respectively. From the ×250 magnification images, the 0F and 3F-DLC show peel-off on the worn edge. This type of failure is attributed to the high hardness and intrinsic stress of the film. It was discussed by previous research that the intrinsic stress in DLC film is compressive and managed by the sub-implantation growth mechanism, which can be explained in terms of the film structure and ion bombardment throughout the development process [10]. It has been proven by Nobili and Guglielmini, that the F-DLC film displays less stress than the DLC film itself [30]. Previous research also discussed that there are several reasons ascribed to stress reduction [10, 15, 30, 31]. First, when fluorine atoms are added to DLC, hydrofluoric acid (HF) volatile gas is created, which lowers the amount of hydrogen, especially unbound hydrogen. A reduced atomic density has reportedly been shown to reduce quenched-in strain. This refers to the gradual transition from a metastable sp^3 to a stable sp^2 configuration, which reduces the stiffness of the carbon network and, in turn, leads to a reduction in internal stress. Second, the mechanism for energy sharing explained how stress decreased as CF_4 partial pressure rose. Third, fluorocarbon groups, which served as termination radicals, encourage the development of a border in the three-dimensional network, which is advantageous for the reduction of internal stress [30]. In conclusion, when the fluorine concentration increases, stress decreases, showing a trend similar to that of hardness and modulus. In this study, it is estimated that the maximum pressure for all sample is almost the same (SUJ2 ball and DLC disc: 0.43 to 0.42 GPa), the failure is confirmed to be contributed by the reason discussed above.

By comparing the Raman spectroscopy of the coating before and after sliding (analysis in the wear track), it can be seen that the intensity of the peaks is relatively the same. This means that the crystal structure of the coating is relatively the same despite the peel-off on the edge as shown in Figs. 9(b, d, and f). Meanwhile, the analysis comparison shows that the position (Fig. 5a), FWHM (Fig. 5b), and intensity ratios (Fig. 5c) of D and G peaks for all coatings are almost the same before and after sliding. Hence, it can be said that there were no changes in sp^3/sp^2 ratios. These findings correlate with the SEM image obtained where the DLC failed through peeling off instead of breakage of the Van der Waals bond.

4 Conclusions

Fluorine-doped DLC (F-FLC) film was deposited on SUS304 using a Plasma Enhanced Chemical Vapor Deposition (PECVD) method. The surface properties were determined by using nano-indenter, contact angle, and Raman spectroscopy for the hardness and Young's modulus, hydrophobicity, and chemical bonding respectively meanwhile the tribological behavior was analyzed by using a dry sliding ball-on-disc tribometer. The major findings are drawn as follows:

(1) Both the hardness and Young's modulus of the films decrease as the fluorine content increases. The hardness is maximum when there is no CF_4 gas feed and minimum when the CF_4 gas is fed at 10 sccm.
(2) The presence of water-adsorbed layer leads to a viscous drag and even capillary forces, thus increasing the adhesion and friction of the film surface. With the increases of F elements in the film, the COF decreases. However, due to hydrophobicity, the very little formation of water adsorption layer caused the 10F-DLC starts with a relatively high COF before decreasing as the rotation increased.
(3) Worn surface observations show DLC film without F possessed severe wear compared to F-DLC film with peel-off observed along the edge of the film.

Acknowledgements

This research was funded by Universiti Teknologi Malaysia through the Post-Doctoral Fellowship Scheme Grant number: Q.K130000.21A2.05E39 and UTM Fundamental Research: Q.K130000.3843.22H20. The authors also acknowledge the support provided by the Tribology and Precision Machining i-Kohza (TriPreM) for the financial, facility, and equipment provided.

References

[1] Zhao X, Lu Z, Wu G, Zhang G, Wang L, Xue Q. Preparation and properties of DLC/MoS_2 multilayer coatings for high humidity

tribology. Mater Res Express. 2016;3(6): 066401.
[2] Vetter J. 60 years of DLC coatings: Historical highlights and technical review of cathodic arc processes to synthesize various DLC types, and their evolution for industrial applications. Surface and Coatings Technology. 2014;257: 213-240.
[3] Singh RK, Xie ZH, Bendavid A, Martin PJ, Munroe P, Hoffman M. Effect of substrate roughness on the contact damage of DLC coatings. Diamond and Related Materials. 2008;17(6): 975-979.
[4] Ronkainen H, Varjus S, Holmberg K. Tribological performance of different DLC coatings in water-lubricated conditions. Wear. 2001;249(3-4): 267-271.
[5] Suzuki M, Ohana T, Tanaka A. Tribological properties of DLC films with different hydrogen contents in water environment. Diamond and Related Materials. 2004;13(11-12): 2216-2220.
[6] Ronkainen H, Varjus S, Koskinen J, Holmberg K. Differentiating the tribological performance of hydrogenated and hydrogen-free DLC coatings. Wear. 2001;249(3-4): 260-266.
[7] Jiang J, Arnell RD. The effect of substrate surface roughness on the wear of DLC coatings. Wear. 2000;239(1): 1-9.
[8] Tanaka A, Nishibori T, Suzuki M, Maekawa K. Tribological properties of DLC films deposited using various precursors under different humidity conditions. Diamond and Related Materials. 2003;12(10-11): 2066-2071.
[9] Zhong M, Zhang C, Luo J. Effect of substrate morphology on the roughness evolution of ultra thin DLC films. Applied Surface Science. 2008;254(21): 6742-6748.
[10] Zhang L, Wang F, Qiang L, Gao K, Zhang B, Zhang J. Recent advances in the mechanical and tribological properties of fluorine-containing DLC films. RSC Advances. 2015;5(13): 9635-9649.
[11] Dalibón EL, Heim D, Forsich C, Rosenkranz A, Guitar MA, Brühl SP. Characterization of thick and soft DLC coatings deposited on plasma nitrided austenitic stainless steel. Diamond and Related Materials. 2015;59: 73-79.
[12] Bendavid A, Martin PJ, Randeniya L, Amin MS, Rohanizadeh R. The properties of fluorine-containing diamond-like carbon films prepared by pulsed DC plasma-activated chemical vapour deposition. Diamond and Related Materials. 2010;19(12): 1466-1471.
[13] Akaike S, Kobayashi D, Aono Y, Hiratsuka M, Hirata A, Hayakawa T, Nakamura Y. Relationship between static friction and surface wettability of orthodontic brackets coated with diamond-like carbon (DLC), fluorine- or silicone-doped DLC coatings. Diamond and Related Materials. 2016;61: 109-114.
[14] Yao ZQ, Yang P, Huang N, Sun H, Wang J. Structural, mechanical and hydrophobic properties of fluorine-doped diamond-like carbon films synthesized by plasma immersion ion implantation and deposition (PIII-D). Applied Surface Science. 2004;230(1-4): 172-178.
[15] Zhang L, Wang J, Zhang J, Zhang B. Increasing fluorine concentration to control the microstructure from fullerene-like to amorphous in carbon films. RSC Advances 2016;6(26): 21719-21724.
[16] Jongwannasiri C, Yoshida S, Watanabe S. Effects of fluorine and silicon incorporation on tribological performance of diamond-like carbon films. Materials Sciences and Applications. 2019;10(3): 170-185.
[17] Fukuda K. Combinational analysis of multi-data obtained in a repeated sliding system. Wear. 2008;264(7-8): 499-504.
[18] Yap KK, Fukuda K, Vail JR, Wong J, Masen MA. Spatiotemporal mapping for in-situ and real-time tribological analysis in polymer-metal contacts. Tribology International. 2022;171: 107533.
[19] Wang Y, Xu J, Zhang J, Chen Q, Ootani Y, Higuchi Y, Ozawa N, Martin JM, Adachi K, Kubo M. Tribochemical reactions and graphitization of diamond-like carbon against alumina give volcano-type temperature dependence of friction coefficients: A tight-binding quantum chemical molecular dynamics simulation. Carbon. 2018;133: 350-357.
[20] Ferrari AC, Robertson J. Interpretation of raman spectra of disordered and amorphous carbon. Physical Review B. 2000;61(20): 14095-14107.
[21] Ferrari AC, Basko DM. Raman spectroscopy as a versatile tool for studying the properties of graphene. Nature Nanotechnology. 2013;8(4): 235-246.
[22] Casiraghi C, Ferrari AC, Robertson J. Raman spectroscopy of hydrogenated amorphous carbons. Physical Review B. 2005;72(8): 085401.
[23] Saito R, Hofmann M, Dresselhaus G, Jorio A, Dresselhaus MS. Raman spectroscopy of graphene and carbon nanotubes. Advances in Physics. 2011;60(3): 413-550.
[24] Ferrari AC, Meyer JC, Scardaci V, Casiraghi C, Lazzeri M, Mauri F, Piscanec S, Jiang D, Novoslov KS, Roth S, Geim AK. Raman spectrum of graphene and graphene layers. Physical Review Letters. 2006;97(18): 187401.
[25] Shinde SM, Kano E, Kalita G, Takeguchi M, Hashimoto A, Tanemura M. Grain structures of nitrogen-doped graphene synthesized by solid source-based chemical vapor deposition. Carbon. 2016;96: 448-453.
[26] Basko DM. Theory of resonant multiphonon raman scattering in graphene. Physical Review B. 2008;78: 125418.
[27] Chen CF, Park CH, Boudouris BW, Horng J, Geng B, Girit C, Zettl A, Crommie MF, Segalman RA, Louie SG, Wang F. Controlling inelastic light scattering quantum pathways in graphene. Nature. 2011;471(7340): 617-620.
[28] Wang J, Ma J, Huang W, Wang L, He H, Liu C. The investigation of the structures and tribological properties of F-DLC coatings deposited on Ti-6Al-4V alloys. Surface and Coatings Technology. 2017;316: 22-29.
[29] Manaf ND, Fukuda K, Subhi ZA, Mohd Radzi MF. Influences of surface roughness on the water adsorption on austenitic stainless steel. Tribology International. 2019;136: 75-81.
[30] Nobili L, Guglielmini A. Thermal stability and mechanical properties of fluorinated diamond-like carbon coatings. Surface and Coatings Technology. 2013;219: 144-150.
[31] Hasebe T, Matsuoka Y, Kodama H, Saito T, Yohena S, Kamijo A, Shiraga N, Higuchi M, Kuribayashi S, Takahashi K, Suzuki T. Lubrication performance of diamond-like carbon and fluorinated diamond-like carbon coatings for intravascular guidewires. Diamond and Related Materials. 2006;15(1): 129-132.